Turkish Journal of Electrical Engineering & Computer Sciences

http://journals.tubitak.gov.tr/elektrik/

Research Article

Turk J Elec Eng & Comp Sci
(2013) 21: 2110 – 2126

doi:10.3906/elk-1202-21

Swarm optimization tuned Mamdani fuzzy controller for diabetes delayed model

Mohammad Hassan KHOOBAN,[1,*] **Davood NAZARI MARYAM ABADI,**[2]
Alireza ALFI,[3] **Mehdi SIAHI**[2]

[1]Department of Electrical Engineering, Sarvestan Branch, Islamic Azad University, Sarvestan, Iran
[2]Department of Electrical Engineering, Garmsar Branch, Islamic Azad University of Garmsar, Iran
[3]Faculty of Electrical and Robotic Engineering, Shahrood University of Technology, Shahrood, Iran

Received: 06.02.2012 • **Accepted:** 15.06.2012 • **Published Online:** 24.10.2013 • **Printed:** 18.11.2013

Abstract: Diabetes is a chronic disease in which there are high levels of sugar in the blood. Insulin is a hormone that regulates the blood glucose level in the body. Diabetes mellitus can be caused by too little insulin, a resistance to insulin, or both. Although research activities on controlling blood glucose have been attempted to lower the blood glucose level in the quickest possible time, there are some shortages in the amount of the insulin injection. In this paper, a complete model of the glucose–insulin regulation system, which is a nonlinear delay differential model, is used. The purpose of this paper is to follow the glucose profiles of a healthy person with minimum infused insulin. To achieve these purposes, an intelligent fuzzy controller based on a Mamdani-type structure, namely the swarm optimization tuned Mamdani fuzzy controller, is proposed for type 1 diabetic patients. The proposed fuzzy controller is optimized by a novel heuristic algorithm, namely linearly decreasing weight particle swarm optimization. To verify the robust performance of the proposed controller, a group of 4 tests is applied. Insensitivity to multiple meal disturbances, high accuracy, and superior robustness to model the parameter uncertainties are the key aspects of the proposed method. The simulation results illustrate the superiority of the proposed controller.

Key words: Diabetes, fuzzy logic control, linearly decreasing weight particle swarm optimization, Wang model

1. Introduction

The World Health Organization (WHO) apprises that over 180 million people in the world have diabetes and this rate is estimated to reach 360 million people by 2030 [1]. This growth is associated with the increasing average age of society, an increase in obesity, and also probably the increase in the longevity of those with diabetes. The difficulties of diabetes mellitus are far less prevalent and less intense in individuals who have well-controlled blood sugar levels [2,3].

More extensive health difficulties precipitate the detrimental impacts of diabetes. These include smoking, high cholesterol levels, obesity, hypertension, and the absence of orderly exercise. Diabetes mellitus can lead to some side effects such as blindness, hyperglycemia, hypoglycemia, diabetic coma, and respiratory infections. Blindness is one of the most dangerous complications of diabetes, with a morbidity of 50–65 per 100,000 diabetics per year in Europe [4–6]. However, with good care, visual injuries owing to diabetes can be avoided for the overwhelming majority of patients.

Medical sciences have placed more emphasis on prevention, and in the case of illness, only offer general treatment. In recent years, to improve the treatment of diabetes, new instruments have been designed using biomedical engineering; for instance, the insulin pump. The insulin pump is a medical device used for the

*Correspondence: dr.mohammadhassan.khooban@ieee.org

administration of insulin in the treatment of diabetes mellitus, which is also known as continuous subcutaneous insulin infusion therapy. The insulin pump has an application in the treatment of both types of diabetes [7–10], but what is important is the designing of an appropriate controller for the insulin pump. This paper is associated with expanding an enhanced glucose controller for the insulin pump that is according to an optimal fuzzy-proportional-integral (PI) controller.

Recently, considerable attempts have been made in the expansion of control methods that were assumed to be capable of mimicking the β-cell normal capability [11–15]. The majority of them depended on the easy Bergman's model, which may lead to inefficient treatment owing to the fact that this model cannot generally express the oscillatory behavior of the glucose–insulin system. Moreover, despite the good performance of these controllers, they do not have the capabilities to deal with the uncertainties that exist in biological models. Furthermore, the classical controllers cannot appropriately counter nonlinear and complex systems. As a result, if these controllers are used in practice, it is likely that they would fail when being applied to an actual patient.

In recent years, researchers have extensively used fuzzy logic for the modeling, identification, and control of highly nonlinear dynamic systems [16]. During a set of comparative studies, the advantage of fuzzy controllers over classical controllers has been proven. The purpose of these studies was to hold the blood glucose level at a determined reference point, 4.5 mmol/L, by considering Bergman's minimal model as a model of diabetes mellitus. In [17], a comparative study between the ordinary PI-derivative (PID) and a fuzzy logic controller with the assumption of continuous insulin infusion was represented, where both controllers were designed for the purpose of maintaining the blood glucose level at around 60–100 mg/dL before eating and under 140 mg/dL after eating. In [18], a fuzzy controller based on the ordinary PID controller was designed. In [19], the excellence of the fuzzy PI controller over other controllers was shown, where Bergman's minimal model was used. Aside from being the fastest at bringing the glucose concentration back to a desired value, it is also capable of eliminating errors caused by intense initial circumstances and restoring the blood glucose level to its basal amount within a duration of nearly 1 h. In [20], the efficiency of the fuzzy closed-loop controller was compared with the ordinary PID controller in the presence of intense initial conditions, including an unusual meal disturbance, variations in the parameters of the system, and a white noise that indicates a sensor's error. Although the fuzzy controllers demonstrated better efficiency than the other methods, they have some shortages. Among their disadvantages are: 1) their purpose is to preserve the glucose level at a determined reference point rather than mimicking the glucose–insulin dynamics in healthy individuals, and 2) their significant drawback is the lack of systematic methods to define the fuzzy rules and fuzzy membership functions. Most fuzzy rules are based on human knowledge and differ among people, despite the same system performance. On the other hand, it is difficult to assume that the given expert's knowledge captured in the form of the fuzzy controller leads to optimal control. Hence, the effective approaches for tuning the membership function and control rules without a trial and error method are significantly required.

Motivated by the aforementioned research, the purpose of this paper is to present a novel optimal fuzzy PI controller for stabilizing the blood glucose concentration of type 1 diabetic patients, where a Mamdani-type of fuzzy controller is designed based on a generalized mathematical nonlinear delay differential model of glucose–insulin. This model, with scheduled insulin infusion, demonstrates glucose status in healthy people [21]. The optimized controller is also designed in a way that the glucose oscillation under its control mimics that of the reference model. To achieve this objective, linearly decreasing inertia weight particle swarm optimization (LDW-PSO), which is an improved algorithm of PSO, is employed to choose the best parameter amounts of the inputs and the output fuzzy membership functions, as well as the closed-loop weighting factors.

Recently, the PSO algorithm has been become available and there have been promising techniques introduced for real-world optimization problems [22]. Compared to the genetic algorithm (GA), PSO takes less time for each function evaluation as it does not use many of the GA operators like mutation, crossover, and selection operator [23]. Due to the simple concept, easy implementation, and quick convergence, nowadays PSO has gained much attention and wide applications in different fields [24]. The rest of this paper is organized as follows. In the next section, the mathematical model of the glucose insulin regulatory system in a type 1 diabetes mellitus patient is introduced and details of the proposed control are then presented. The simulation results of the proposed control system with discussions are then presented and, finally, the conclusions are drawn.

2. Glucose–insulin model

Insulin treatments are frequently presented based on clinical trials; however, mathematical models have been considered for some special conditions. A delay differential equation model to simulate the pancreatic insulin secretion with exogenous insulin infusion was proposed by Wang et al. [21]. This model was studied analytically and numerically. The existence and stability of intermittent solutions was also proven. In addition, the behavior of the system, under intermittent exogenous glucose infusion and insulin infusion, was studied.

The insulin and the glucose dynamics under insulin treatment from outside the body for a type 1 diabetic patient are shown as follows [21]:

$$\frac{dG}{dt} = G_{in}(t) - f_2(G(t)) - f_3(G(t))f_4(I(t-\tau_3)) + f_5(I(t-\tau_2)), \tag{1}$$

$$\frac{dI}{dt} = I_{in}(t) - d_i(I(t)), \tag{2}$$

where$G(t)$ and $I(t)$ represent the plasma glucose and the insulin concentrations at time t ≥ 0, respectively. And $G_{in}(t)$ and $I_{in}(t)$ denote the glucose absorption rate and the exogenous insulin infusion rate, respectively, as shown in Figures 1 and 2. Finally, d_i is the clearance rate parameter.

$$G_{in}(t) = \begin{cases} 0.05 + \frac{5}{15t} & 0 \leq t < 15\,(\text{min}) \\ 0.05 + 5\frac{45-t}{45-15} & 15 \leq t < 45\,(\text{min}) \\ 0.05 & 45 \leq t \leq 240\,(\text{min}) \end{cases} \tag{3}$$

$$I_{in}(t) = \begin{cases} 0.25 & 0 \leq t \leq 5(\text{min}) \\ 0.25 + (1 + \frac{t-30}{30-5}) & 5 \leq t < 30(\text{min}) \\ 0.25 + (1 - \frac{t-30}{120-30}) & 30 \leq t < 120(\text{min}) \\ 0.25 & 120 \leq t < 240(\text{min}) \end{cases} \tag{4}$$

$f_2(G(t))$ given in Eq. (5) is the insulin-independent exploitation of glucose mostly by brain and nerve cells. The term $f_3(G(t))\, f_4(I(t))$ demonstrates the insulin-dependent exploitation of the glucose owing to muscle, fat, and other tissues. The corresponding formulations of these functions are presented in Eqs. (6) and (7), respectively; g $\tau_z > 0$ is the time delay for insulin-dependent glucose exploitation by cells and $\tau_y > 0$ is the hepatic glucose generation delay. $f_5(I(t))$ given in Eq. (8) shows the glucose generation function regulated by the glucose concentration. The insulin decomposition is proportional to the insulin concentration by parameter d_i, in which $d_i > 0$.

$$f_2(G(t)) = U_b(1 - exp(-G/(C_2V_g))) \tag{5}$$

$$f_3(G(t)) = \frac{G}{C_3 * V_g} \tag{6}$$

$$f_4(I(t)) = U_0 + (U_m - U_0)/(1 + exp(-\beta ln(I/C_4(1/V_i + 1/(0.2t_i))))) \tag{7}$$

$$f_5(I(t)) = Rg/(1 + exp(\hat{\alpha}(I/Vp - C_5))) \tag{8}$$

In above equations, U_b, C_2, V_g, C_3, U_0, U_m, β, C_4, V_i, t_i, R_g, α, V_p, and C_5 are fixed quantities.

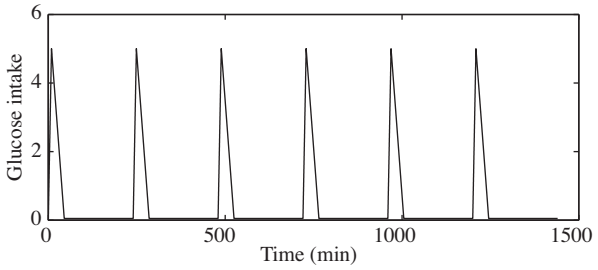

Figure 1. The glucose absorption rate (mg dL^{-1} min^{-1}).

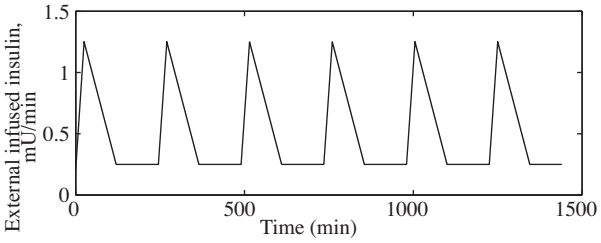

Figure 2. The exogenous insulin infusion rate (mU/min).

3. Dynamic model of the micropump of insulin infusion

The dynamic model of the micropump of insulin infusion was given in [25]. The unloaded volume variation can be stated as:

$$\Delta V = \frac{3r^4(5 + 2\mu)(1 - \mu)dU}{4h^2(3 + 2\mu)}, \tag{9}$$

where U is the voltage applied to the lead zirconate titanate (PZT) film with piezoelectric factor d. The thickness of the film is $h\mu$m and the radius is $r\mu$m. μ is the Poisson ratio. Note that the volume variation is in proportion to the voltage variation applied to the PZT film. This proportion can be written as follows:

$$\Delta V = K\Delta U, \tag{10}$$

where K is the coefficients of Eq. (9). The objective of the micropump is to alter the operating voltage between zero and a positive amount, with the difference in voltage by ΔU. Next, the insulin infusion rate is obtained as:

$$Q = Kf\Delta U, \tag{11}$$

where f is the operating frequency of the micropump.

4. PSO algorithm

The PSO algorithm is a relatively novel population-based heuristic optimization technique that is based on a metaphor of social interaction, namely bird flocking. The key advantages of PSO are: 1) the objective function's gradient is not required, 2) PSO is more flexible and robust in comparison with traditional optimization methods, 3) PSO ensures the convergence to the optimal solution, and 4) compared to the GA, PSO takes less time for each function evaluation as it does not use many of the GA operators, like mutation, crossover, and selection operator.

In PSO, each candidate solution is called a 'particle'. Each particle in the swarm represents a candidate solution to the optimization problem, and if the solution is made up of a set of variables, the particle can

correspondingly be a vector of variables. In PSO, each particle is flown through the multidimensional search space, adjusting its position in the search space according to its momentum and both individual and global memories. Therefore, the particle makes use of the best position encountered by itself and that of its neighbors to position itself toward an optimal solution. The fitness of each particle can be evaluated according to the objective function of the optimization problem. At each iteration, the velocity of every particle will be calculated as follows:

$$v_i(t+1) = \omega v_i(t) + c_1 r_1(P_{id} - x_i(t)) + c_2 r_2(P_{gd} - x_i(t)), \tag{12}$$

where $x_i(t)$ is the current position of the particle, P_{id} is the best of the solutions that this particle has reached, and P_{gd} is one of the best solutions. After calculating the velocity, the new position of each particle can be worked out:

$$x_i(t+1) = x_i(t) + v_i(t+1). \tag{13}$$

The PSO algorithm is repeated using Eqs. (12) and (13), which are updated at each iteration, until the prespecified number of generations is reached.

Although the standard PSO (SPSO) involves some important advances by providing high-speed convergence in specific problems, it does exhibit some shortages. It is found that SPSO has a poor ability to search for a fine particle because it lacks a velocity control mechanism. Many approaches have been attempted to improve the performance of SPSO by variable inertia weight. The inertia weight is critical for the performance of PSO, which balances the global exploration and local exploitation abilities of the swarm. A big inertia weight facilitates exploration, but it makes the particle take a long time to converge. Conversely, a small inertia weight makes the particle converge faster, but it sometimes leads to a local optimum. Hence, there are several PSO algorithms with an adaptive inertia weight, such as LDW-PSO, nonlinearly decreasing weight PSO (NLDW-PSO), or time varying inertia weight PSO [26]. To choose the most appropriate one, several factors must be considered depending on the problem in hand. The computational time is a very important factor in our application and it should not be a big issue for the implementations. Compared with above mentioned algorithms, LDW-PSO demonstrates its superiority in the computational complexity, success rate, and solution quality. Hence, the LDW-PSO algorithm is used in this paper. In NLDW-PSO, the inertia weight is adapted linearly as follows [27]:

$$\omega(t) = \omega_{\min} + \frac{iter_{\max} - t}{iter_{\max}}.(\omega_{\max} - \omega_{\min}), \tag{14}$$

where $iter_{\max}$ is the maximal number of iterations, and $t$is the current number of iterations. As iterations go, therefore, ω decreases linearly from $\omega_{\max}$ to $\omega_{\min}$.

5. The proposed method

5.1. Structure design

The block diagram of the proposed swarm optimization tuned Mamdani fuzzy controller (SOTFC) for the regulation of plasma glucose in type 1 diabetic patients is shown in Figure 3. The controller is structured with a Mamdani-type fuzzy architecture with 2 input linguistic variables and 1 output variable. The input linguistic variables are the error signal (e) and its rate of change ($\dot{e}$), and the output linguistic variable is the exogenous insulin infusion rate ($\Delta \mathrm{I}_{in}$). In fact, the parameter e represents the difference between the measured blood glucose level and the reference glucose level.

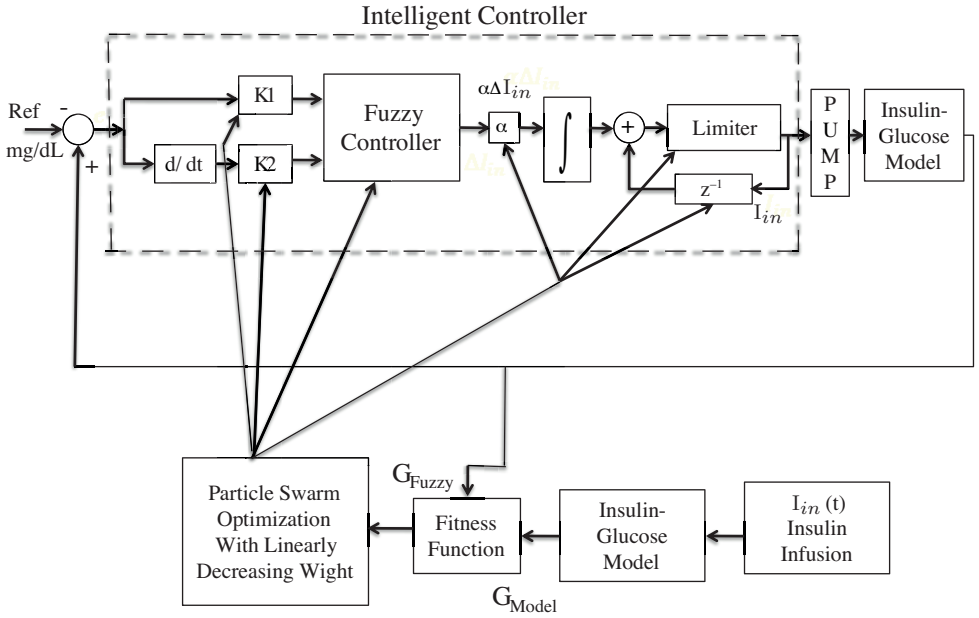

Figure 3. General scheme of the proposed controller (SOTFC).

The key components of a fuzzy logic controller are the fuzzifier, the inference engine, the rule base, and the defuzzifier, as shown in Figure 4. The fuzzifier transforms the numeric into fuzzy sets, and so this operation is called fuzzification. The inference engine is the main component of the fuzzy logic controller, which performs all of the logic manipulations in a fuzzy controller. The rule base consists of membership functions and control rules. Finally, the results of the inference process, which is an output represented by a fuzzy set, is transformed into a numeric value using the defuzzifier, and this operation is called defuzzification. The membership functions of the fuzzy controller consist of 3 and 5 membership functions for the inputs' linguistic variables (e and $\dot{e}$) and the output's linguistic variable ($\Delta \mathrm{I}_{in}$), respectively. The general shape of the membership functions are as follows:

$$\mu(z) = \exp\left(\frac{(z-c)^2}{2\sigma}\right), \tag{15}$$

where the parameter c is the mean and the parameter σ is the variance of each membership function, the parameter z is the crisp input amount to be fuzzified, and $\mu(z)$ is its membership function grade with numerical value in the interval [0 1].

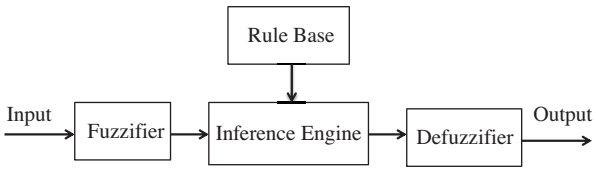

Figure 4. Components of a fuzzy logic controller.

The linguistic meanings of the input and output membership functions are listed in Tables 1 and 2, respectively. By the definition of the input and output fuzzy sets, a total of 9 IF-THEN rules are defined. These rules are listed in Table 3.

In designing the fuzzy controller, using the submin compositional rule of inference, the AND fuzzifier, and the center of gravity defuzzifier, the crisp output can be defined as

$$Z^* = \frac{\int \mu_C(z) \,.\, z\, dz}{\int \mu_C(z)\, dz}, \tag{16}$$

where $\int$ indicates an algebraic integration. The defuzzified amount goes through an output restrictive and then to an insulin pump.

Table 1. Label of input membership functions.

Label	N	Z	P
Meaning	Negative	Zero	Positive

Table 2. Label of output membership functions.

Label	NL	NS	Z	PS	PL
Meaning	Negative large	Negative medium	Zero	Positive medium	Positive large

Table 3. Fuzzy IF-THEN rules.

de/dt e	N	Z	P
N	NL	NS	Z
Z	NS	Z	PS
P	Z	PS	PL

In the fuzzy inference engine, if the antecedent part is performed by the MIN operator, the output fuzzy set related to every fuzzy rule R_i will be cut at α_i. The overall inference $\mu_c(\Delta I_{in})$ can be achieved as follows [28]:

$$\mu_c(\Delta I_{in}) = \mu_{c1} U \mu_{c2} ... \mu_{c9}, \tag{17}$$

where μ_{ci} is the inference result derived from rule i. In this paper, the aggregation part is done by the SUM operator.

It is noticeable that due to the saturation that exists in each actuator, a limiter is added to the output of the controller. It avoids the wind-up and wind-down effects, which protects the body against the increasing or decreasing of the insulin injection dose. Hence,

$$\Delta I_{in} = \alpha \Delta I_{in}(defuz_*(fuz(K_{1*}e, K_{2*}\dot{e}))), \tag{18}$$

where *defuz* and *fuz* denote the defuzzification and the fuzzification operations, respectively. K_1, K_2, and $\alpha\Delta I_{in}$ are also the scale gains of the error, the error rate, and the output, respectively. The overall output of the controller is stated as follows:

$$I_{in}(G(t)) = \begin{cases} U & I_{in} \geq U \\ I_{in}(G(t\,1)) + \Delta I_{in}(G(t)) & U < I_{in} < L \\ L & I_{in} \leq L \end{cases}, \tag{19}$$

where $I_{in}(G(t))$ and $I_{in}(G(t-1))$ demonstrate the current and the previous exogenous insulin quantities at $G(t)$ and $G(t-1)$, respectively. $\Delta I_{in}(G(t))$ represents an increment or decrement in the insulin injection due

to the glucose concentration. Finally, U and L are the upper and the lower limitations of the saturation block, respectively. This means that the proposed fuzzy controller works in the interval [L,U] mU/min and saturates outside of this range. Insulin is injected into the body by insulin pump through a needle. Due to the thinness of the insulin pump's needle there are limitations in the insulin infusion rate. Indeed, the limiter represents the limitations of the insulin infusion rate. Figures 5 and 6 describe the effect of the limiter, where it can be seen that the limiter is capable of keeping the insulin infusion rate in a specified range. We can also see that in the absence of a limiter, wind-up and wind-down effects occur. The wind-down effect will lead to hyperglycemia and the wind-up effect will lead to hypoglycemia.

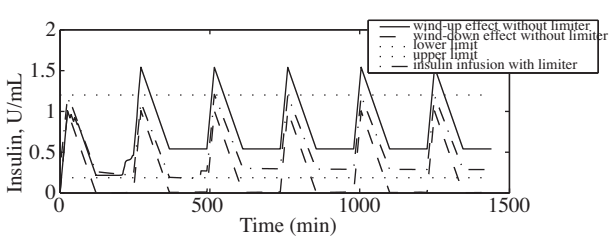

Figure 5. Effect of the limiter in insulin infusion rate.

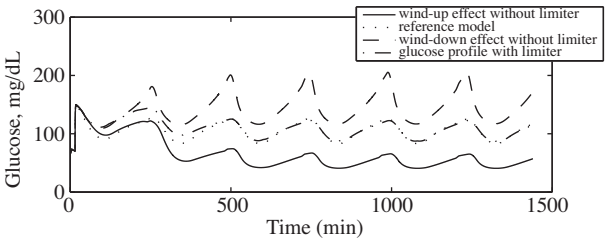

Figure 6. Effect of the limiter in hyperglycemia and hypoglycemia.

From Eq. (19), at $t = 0$, the overall quantity of the insulin can be obtained as:

$$I_{in}(G(0)) = \Delta I_{in}(G(0)) + IC. \tag{20}$$

Here, the parameter IC is the quantity of injected insulin from the pump at t = 0. This parameter increases the speed response in the tracking of the reference model. Moreover, the parameter α_i, called the matching level of every fuzzy rule, is computed. For instance, the matching level of rule 1 can be achieved by the following:

$$\alpha_1 = \mu_N(e) \cap \mu_N(\dot{e}), \tag{21}$$

where α_1 is the matching level of R_1 and $\mu_N(e)$ and $\mu_N(\dot{e})$ are the membership function grades of the crisp inputs (e) and $(\dot{e})$, respectively. The symbol $\cap$ represents the AND operator, which is considered to be the product operator. In the next section, the implementation of the SOTFC will be illustrated.

5.2. Implementation

As mentioned before, the goal of the SOTFC is to mimic the normal behavior of glucose and insulin as characterized by the reference model, not to lower the blood glucose level to a specified preset glucose amount as described in [17–20]. Based on this, LDW-PSO is employed for tuning the parameters of the input and output membership functions, as defined in Eq. (15), and the weighting parameters, i.e. K_1, K_2, and $\alpha\Delta I_i$. To set the best limit on the exogenous insulin infusion, the parameters U and L are also determined by LDW-PSO. In addition, to determine the best value of the insulin, injected at the start of the simulation, the parameter IC is obtained by LDW-PSO.

Before proceeding with the optimization operations, a performance criterion should be defined first. In general, a heuristic algorithm such as PSO only needs to evaluate the fitness function to guide its search and there is no requirement for derivatives about the system. In this paper, the absolute percentage error is

considered. Thus, the fitness function is defined as follows:

$$J = \frac{1}{n}\sum_{t=0}^{n}\left|\frac{G_{Model} - G_{Fuzzy}}{G_{Model}}\right|, \tag{22}$$

where G_{Model} is the glucose amount obtained by the reference model, G_{Fuzzy} represents the real output of glucose–insulin system (see Figure 3), and n is the duration of simulation.

6. Simulation results

In order to demonstrate the performance of the SOTFC, simulations are carried out in 2 parts: with and without the uncertainty. To simulate the SOTFC, MATLAB software is applied. The numerical values of the glucose–insulin model's parameters are listed in Table 4. Simulation results have been gained for 100 runs of particles considered during a period of 1440 min (24 h). The parameters of LDW-PSO are also listed in Table 5.

Table 4. The parameters of the glucose–insulin model [21].

Parameters	Units	Values	Parameters	Units	Values
Vg	1	10	U_0	mg min^{-1}	40
U_b	mg min^{-1}	72	U_m	mg min^{-1}	940
C_2	mg 1^{-1}	144	B	1	1.77
C_3	mg 1^{-1}	1000	C_4	mU 1^{-1}	80
V_p	1	3	R_g	mg min^{-1}	180
V_i	1	11	$\hat{\alpha}$	1 mU^{-1}	0.29
t_i	min	100	C_5	mU 1^{-1}	26

Table 5. The parameters of LDW-PSO.

Size of the swarm	50
Dimension of the problem	28
Maximum number of iterations	100
Cognitive parameter C_1	1
Social parameter C_2	1
Construction factor C	1

6.1. Performance analysis without uncertainty

The goal of the optimization problem is to set the parameters of the control system so that the glucose profile by the SOTFC is very close to that of the reference model, as shown in Figure 7. As shown in [29], the membership functions with various averages and constant variances have better performance in mimicking the blood glucose response of the reference model. Thus, the variance of all Gaussian membership functions is set to 0.3.

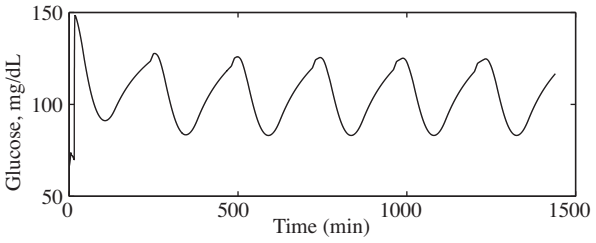

Figure 7. Glucose profile of the reference model.

The average of membership functions with the linguistic variables NL, NS, and N are defined on the interval [–1 0], whereas the linguistic variables PL, PS, and P are defined on the interval [0 1]. The average of linguistic variable Z is also on the interval [–0.5 0.5]. Finally, the parameters K_1, K_2, $\alpha\Delta I_{in}$, U, L, and IC are defined on the intervals [0 0.5], [0 0.5], [0 0.5], [0.5 2], [0 0.45], and [0 2], respectively. The search space is considered because of the authors' knowledge about the problem at hand, such that the optimum values exist in these intervals. The obtained membership functions of the inputs and the output are shown in Figures 8–10, respectively. Figure 11 shows the output surface of the controller.

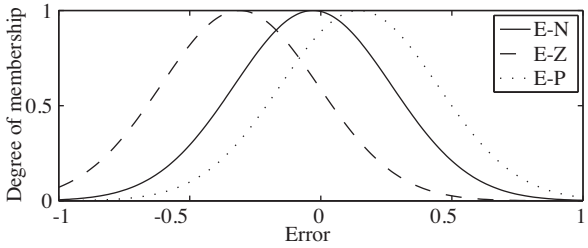

Figure 8. Obtained membership functions of input 1.

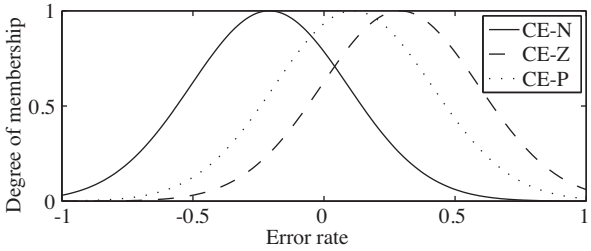

Figure 9. Obtained membership functions of input 2.

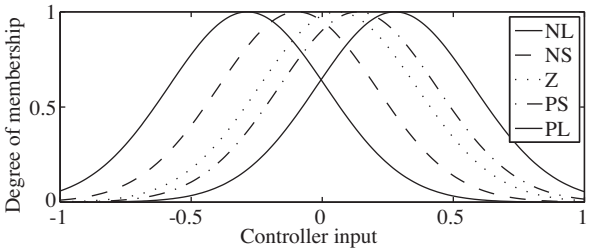

Figure 10. Obtained membership functions of the output (infused insulin).

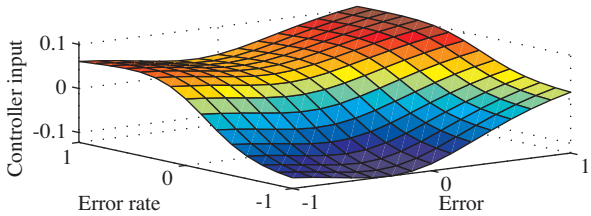

Figure 11. Control surface.

The difference between the glucose and insulin profile of both the reference model and the SOTFC is represented in Figures 12 and 13, respectively. Moreover, the closed-loop control parameters obtained by LDW-PSO are listed in Table 6. Finally, in order to show the feasibility of the SOTFC, the results are compared with those obtained in [29], which is summarized below:

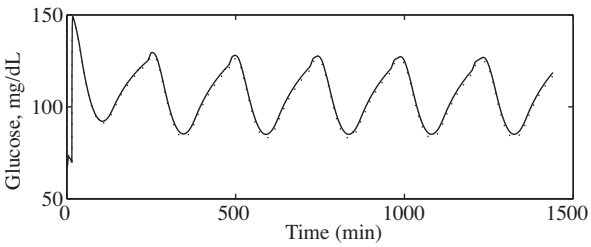

Figure 12. Glucose profile with SOTFC (-) and the reference model (.).

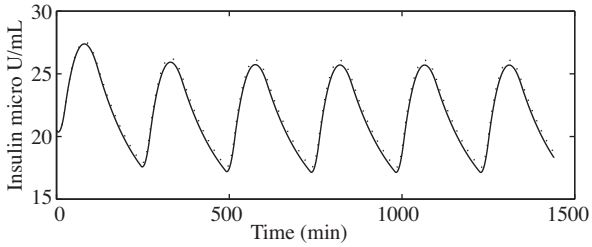

Figure 13. Insulin profile with SOTFC (-) and the reference model (.).

1) The SOTFC in this paper is much less complicated. As shown in Table 3, the designed controller in this paper has only 9 rules, and with these limited rules, the design requirements are satisfied. In [29], however,

for achieving satisfactory results, 49 rules were defined.

2) The controller has better performance. As shown in Table 7, the fitness function value is 1.235%, while in [29], the best obtained value for this parameter was 1.3787%. Moreover, as shown in Table 7, the average value of the glucose obtained in this paper is 107.4 mg/dL, while the best value of this parameter obtained in [29] was 106.3488 mg/dL. Moreover, Table 7 shows the lower values of the daily infused insulin compared with those obtained in [1].

Table 6. The parameters obtained by LDW-PSO.

Parameter	Value
K_1	0.0358
K_2	0.3236
$\alpha\Delta I_{in}$	0.3180
U (mU/min)	1.2012
L (mU/min)	0.1873
IC (mU/min)	0.1749

Table 7. Comparison of performance analyses.

	SOTFC	Controller presented in [29]	Reference model
Fitness function value	1.235%	1.3787%	-
Average value of glucose	104.6055 (mg dL^{-1} min^{-1})	106.3488 (mg dL^{-1} min^{-1})	107.38 (mg dL^{-1} min^{-1})
Daily infused insulin	707.595 (mU/min)	708.8412 (mU/min)	705.25 (mU/min)

6.2. Performance analysis with uncertainty

The important part in the design procedure is robustness analysis. In order to demonstrate the robustness of the SOTFC, 4 general cases are taken into account: 1) uncertainty in the clearance rate parameter, 2) changes in the glucose intake profile, 3) unusual glucose intake, and 4) error in the measurement of sensor. Moreover, to illustrate the superiority of the SOTFC, the results in each case are compared with those obtained in [29]. It is necessary to recall that we consider acceptable plasma glucose to be in the range of 60–140 mg/dL, as stated in [17].

6.2.1. Uncertainty in the clearance rate parameter

The clearance rate parameter shows the existing difference between patients in terms of insulin absorption. If this parameter is increased, the insulin degradation rate increases and vice versa. In this part, for simulation of the existing differences between patients in terms of their insulin absorption, the clearance rate parameter given in Eq. (2) is considered to be uncertain, whereas its variation $\hat{d}_i$ is considered to be up to 20% according to the following equation:

$$\hat{d}_i = d_i(1 \pm 20\%), \tag{23}$$

where the nominal value of parameter d_i is 0.0076. The results are illustrated in Figures 14–17. Using the upper bound of $\hat{d}_i$, i.e. $d_i(1+20\%)$, the insulin concentration degrades fast. In this condition, the reference model is unable to preserve the glucose concentration in the allowable range. Consequently, the patients with

this clearance rate value will face high glucose concentrations. This means that hyperglycemia occurs. This state happens because the exogenous insulin infusion depends on a time with a preset value (705.24 mU/day). This value is insufficient to deal with such a situation. Therefore, the insulin concentration of the plasma is very low, as demonstrated in Figure 15, which leads to an increasing of the blood glucose concentration. Because of this, more insulin is required for lowering the blood glucose level. In this case, 826.9351 mU/day of insulin is injected by the insulin infusion pump. However, under the same conditions, 832.3450 mU/day of insulin is infused by the SOTFC in [29]. This shows the advantage of the SOTFC. It is noticeable that almost 1 h after the start, the blood glucose concentration has reached the interval [73.4844 127.3854] mg/dL, which is in the acceptable range.

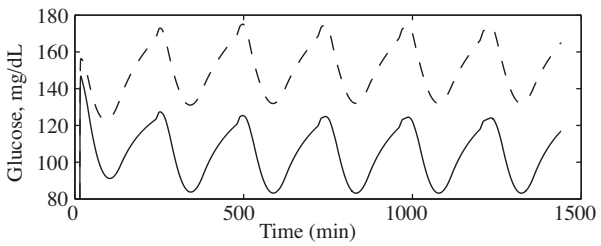

Figure 14. Glucose profile with SOTFC (-) and the reference model (–) using the upper bound of $\hat{d}_i$.

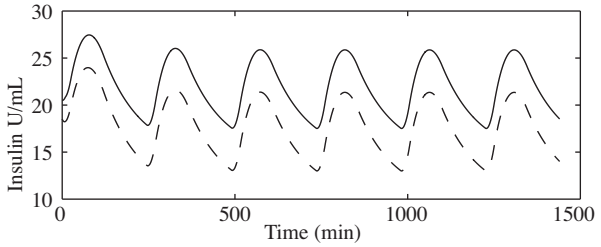

Figure 15. Insulin profile with SOTFC (-) and the reference model (–) using the upper bound of $\hat{d}_i$.

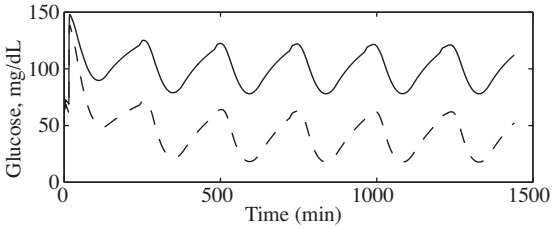

Figure 16. Glucose profile with SOTFC (-) and the reference model (–) using the lower bound of $\hat{d}_i$.

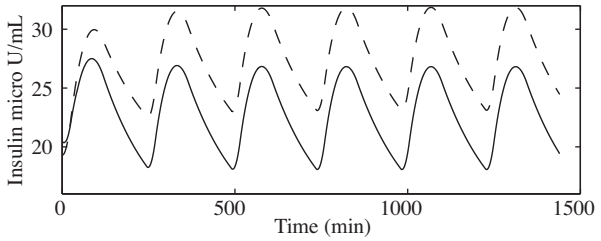

Figure 17. Insulin profile with SOTFC (-) and the reference model (–) using the lower bound of $\hat{d}_i$.

Using the lower bound of $\hat{d}_i$, i.e. $d_i(1-20\%)$, the insulin concentration degrades very slowly. Nearly 1 h after the beginning of the simulation, the insulin concentrations in the reference model and the SOTFC are [23.0001 31.7970] and [18.2476 26.9122], respectively. It is obvious that the insulin concentration of the reference model is greater than that of the controller. This occurs because the amount of insulin injected by the controller (597.8805 mU/day) is less than that injected by the model. However, under similar circumstances, 601.2317 mU/day of insulin was injected by the controller in [29]. This demonstrates the excellence of the SOTFC in this paper. Therefore, the controller is capable of preserving a blood glucose level within the range of [89.7668 125.1513], which is in the acceptable range, whereas without using the controller, the glucose concentration is reduced to less than 60 mg/dL at most moments of the simulation. In this case, the patient is faced with a reduced blood glucose concentration, i.e. hypoglycemia. Referring to Figures 16 and 17, it can be concluded that the SOTFC is capable of dealing with the existing uncertainties in the parameters of the model and preserving the glucose concentration in the acceptable range.

6.2.2. Uncertainty in profile of glucose intake

In this case, it is assumed that the patient eats food 6 times a day and the total time of glucose consumption is 4 h. These assumptions have been done to verify the performance of the SOTFC in confronting large-sized meals. The glucose intake profile given in Eq. (3) and demonstrated in Figure 1 is substituted by the new profile $G_{in-large}$ given in Eq. (24). Figure 18 depicts this profile. In this case, the glucose value received by the new glucose profile equals 9 times that of the reference model.

$$G_{in-large}(t) = \begin{cases} 0.01t^2 & 0 \le t < 120 \text{ (min)} \\ 0.01 + 120 \le t \le 240 \text{ (min)} \\ (120 - (t - 120))^2 \end{cases} \tag{24}$$

$G_{in-large}$ is overstated to confirm that the SOTFC can cope appropriately with large extent meals. In addition, the controller's ability to deal with other glucose inputs is investigated. Figures 19 and 20 represent the glucose and the insulin profiles resulting from large glucose input, respectively. An hour and a half after the start of the simulation, the glucose concentration by the controller reaches the range of [84.6489 122.3334], while in the absence of the controller, the blood glucose level will be increased to the range of [87.4235 130.5369]. This fact demonstrates that the SOTFC is able to maintain the blood glucose level within the acceptable range. Due to the magnitude of the glucose receiving profile, the predetermined amounts of the injected insulin by the reference model are insufficient, and so greater amounts of insulin are injected by the controller. In this case, 732.6526 mU/day of insulin is injected by the SOTFC. However, under the same conditions, 747.9600 mU/day of insulin has been infused by the controller in [29]. On the other hand, this shows the ability of the controller in comparison to the existing controller in [29].

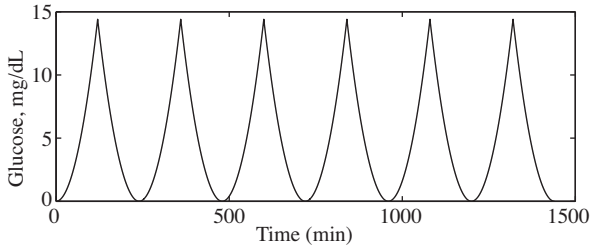

Figure 18. The glucose intake profile given in Eq. (24).

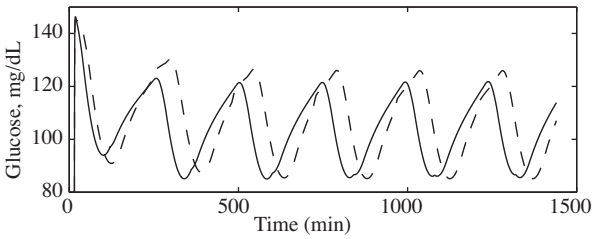

Figure 19. Glucose profile when the glucose intake profile changes. Glucose profile with SOTFC (-) and the reference model (–).

6.2.3. Unusual glucose intake

In this case, the performance of the SOTFC against an unexpected glucose disturbance is evaluated. The highest rate of insulin infusion based on the glucose profile demonstrated in Figure 1 is 5 mg dL^{-1} min^{-1}. In order to simulate the real condition, it is assumed that a patient receives an unusual glucose value $G_{Dis}(t)$ for a duration of 5 min within a certain range of the glucose concentration profile, as follows:

$$G_{Dis}(t) = \begin{cases} 10 & 750 \le t \le 754 \text{ (min)} \\ 0 & otherwise \end{cases} . \tag{25}$$

As can be seen from Eq. (25), the value equal to 10 mg dL^{-1} min^{-1} is added to the model of the glucose intake at the time interval between 750 min and 754 min. This amount is double that of the highest glucose

absorption rate, and the highest rate of total absorbed glucose can approach 15 mg dL^{-1} min^{-1}. Figure 21 confirms that the SOTFC has appropriate performance in dealing with an unusual glucose disturbance. Within the time interval of applying the disturbance, the highest recorded concentration of glucose is 130.9063 mg/dL, which is inside the acceptable limits.

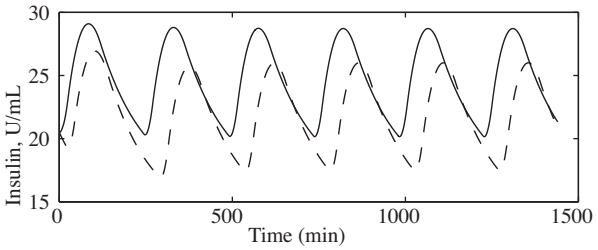

Figure 20. Insulin profile when the glucose intake profile changes. Insulin profile with SOTFC (-) and the reference model (–).

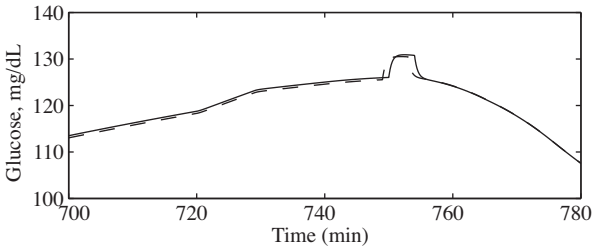

Figure 21. Glucose profile in presence of the disturbance at time interval [750 754] min. Glucose profile with SOTFC (-) and the reference model (–).

6.2.4. Sensor noise

In this case, to consider the effect of measurement noise, a white Gaussian noise with mean equal to 0 and variance equal 0.2 is considered, which is more severe than the conditions shown in [29]. As demonstrated in Figures 22 and 23, the regulated glucose concentration obtained by the SOTFC is [82.1050 124.7336] mg/dL, which is in the acceptable range. This indicates that the SOTFC is robust against the noise of the sensor. Based on the proper performance of the SOTFC, it is very suitable in practical applications such as a miniaturized insulin pump. It is noticeable that to use this controller in real-life applications, the characteristic of the insulin pump must be considered carefully.

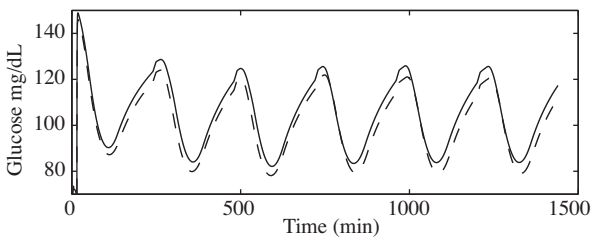

Figure 22. Glucose profile in presence of error noise. Glucose profile with SOTFC (-) and the reference model (–).

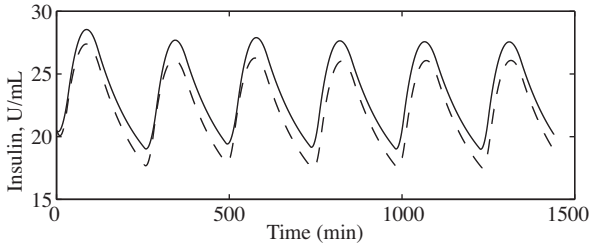

Figure 23. Insulin profile (white Gaussian noise). Insulin profile with SOTFC (-) and the reference model (–).

7. Summary of the simulation results

To verify the robust performance of the SOTFC, a group of 4 tests is considered, including: 1) uncertainty in the clearance rate parameter, 2) changes in the glucose intake profile, 3) unusual glucose intake, and (4) an error in the measurement of the sensor. Uncertainty in the clearance rate parameter leads to states of hyperglycemia or hypoglycemia. As was shown, the SOTFC can appropriately cope with both states and it can keep the blood glucose concentration within the normal range. In the second test, the controller's ability

against high glucose absorption, which is 9 times greater than normal glucose absorption, is evaluated. As was demonstrated, the SOTFC is able to preserve the blood glucose level within the acceptable range. In the third test, for a duration of 5 min, an unusual glucose intake is imposed into the glucose–insulin model. In this test, the SOTFC has appropriate performance in dealing with an unusual glucose disturbance. In the final test, the effect of measurement noise is investigated. To this end, the glucose–insulin model was exposed to a white Gaussian noise. In this case also, the SOTFC is capable of keeping the blood glucose level within the normal range.

8. Conclusion and future works

In this paper, a complete model of the glucose–insulin regulation system, which is a nonlinear delay differential model, was used. The purpose of this paper was to follow the patient glucose profiles of a healthy person with minimum infused insulin. Due to this, a closed-loop control system based on fuzzy logic control for type 1 diabetic patients was proposed. In order to incorporate knowledge about the patient's treatment, the SOTFC was designed using a Mamdani-type fuzzy scheme. In the core of the SOTFC, a heuristic algorithm, namely LDW-PSO, was utilized to optimize the inputs and the output membership function parameters, as well as the closed-loop weighting parameters. Insensitivity to the typical error in commercial devices and multiple meal disturbances, accuracy, robustness to the model parameter variations, and an appropriate settling time are the key aspects of the SOTFC. The simulation results indicated that the SOTFC can successfully tolerate dynamic uncertainty in the patient model while rapidly rejecting meal disturbances and tracking the glucose reference.

To show the superiority of the SOTFC, the results were also compared with the existing controller shown in [29], where the same model for glucose insulin was employed. The comparison demonstrated that the SOTFC is superior to the existing controller in [29] against uncertainties, and it is able to keep the blood glucose level inside the acceptable range. Moreover, the SOTFC mimics the glucose profile of a healthy person perfectly, where the lower value of exogenous insulin infusion is used.

The proposed controller is highly appropriate in feasible applications, like the micropump of insulin infusion, due to its suitable efficiency under different robust tests. The task of the optimal fuzzy controller is primarily to tune the pump's insulin infusion rate due to the glucose concentration by adjusting the voltage applied to the lead PZT film. In fact, the variation of insulin infusion is rated in proportion to the voltage variation applied to the PZT film. Moreover, based on the different dietary habits of patients and their ages and weights, the SOTFC can be readily modified subsequently. Due to the superiority of the type-2 fuzzy controller over the type-1 fuzzy controller in dealing with disturbances and uncertainty, the use of the type-2 fuzzy controller for the insulin pump is recommended in future works.

References

[1] C. Cobelli, C. Dalla Man, G. Sparacino, L. Magni, G. De Nicolao, B.P. Kovatchev, "Diabetes: models, signals, and control", IEEE Reviews in Biomedical Engineering, Vol. 2, pp. 54–96, 2009.

[2] D.M. Nathan, P.A. Cleary, J.Y. Backlund, S.M. Genuth, J.M. Lachin, T.J. Orchard, P. Raskin, B. Zinman, "Intensive diabetes treatment and cardiovascular disease in patients with type 1 diabetes", New England Journal of Medicine, Vol. 353, pp. 2643–2653, 2005.

[3] No authors listed, "The effect of intensive diabetes therapy on the development and progression of neuropathy. The Diabetes Control Complications Trial Research Group", Annals of Internal Medicine, Vol. 122, pp. 561–568, 1995.

[4] T.G. Cormack, B. Grant, M.J. Macdonald, J. Steel, I.W. Campbell, "Incidence of blindness due to diabetic eye disease in Fife 1990-9", British Journal of Ophthalmology, Vol. 85, pp. 354–356, 2001.

[5] M.C. Rhatigan, G.P. Leese, J. Ellis, A. Ellingford, A.D. Morris, R.W. Newton, S.T. Roxburgh, "Blindness in patients with diabetes who have been screened for eye disease", Eye (London), Vol. 13, pp. 166–169, 1999.

[6] C. Trautner, A. Icks, B. Haastert, F. Plum, M. Berger, "Incidence of blindness in relation to diabetes. A population-based study", Diabetes Care, Vol. 20, pp. 1147–1153, 1997.

[7] F.M. Alsaleh, F.J. Smith, S. Keady, K.M. Taylor, "Insulin pumps: From inception to the present and toward the future", Journal of Clinical Pharmacy and Therapeutics, Vol. 35, pp. 127–138, 2010.

[8] I. Conget Donlo, D. Serrano Contreras, J.M. Rodríguez Barrios, I. Levy Mizrahi, C. Castell Abat, S. Roze, "[Cost-utility analysis of insulin pumps compared to multiple daily doses of insulin in patients with type 1 diabetes mellitus in Spain]", Revista Española de Salud Pública, Vol. 80, pp. 679–695, 2006 (article in Spanish).

[9] J. Kesavadev, A. Kumar, S. Ahammed, S. Jothydev, "Experiences with insulin pump in 52 patients with type 2 diabetes in India", [abstract 2021-PO] 68th Scientific Sessions of American Diabetes Association, pp. 78–85, 2008.

[10] J. Kesavadev, S. Balakrishnan, S. Ahammed, S. Jothydev, "Reduction of glycosylated hemoglobin following 6 months of continuous subcutaneous insulin infusion in an Indian population with type 2 diabetes", Diabetes Technology & Therapeutics, Vol. 11, pp. 517– 521, 2009.

[11] L. Kovfics, B. Pal?ncz, "Glucose insulin control of type 1 diabetic patients in $H_2/H\infty$ space via computer algebra", Proceedings of the 2nd International Conference on Algebraic Biology, pp. 95–109, 2007.

[12] L. Magni, D.M. Raimondo, C.D. Man, G. De Nicolao, B. Kovatchev, C. Cobelli, "Model predictive control of glucose concentration in type 1 diabetic patients: an in silico trial", Biomedical Signal Processing and Control, Vol. 4, pp. 338–346, 2009.

[13] G. Marchetti, M. Barolo, L. Jovanovicy, H. Zisser, D.E. Seborg, "An improved PID switching control strategy for type 1 diabetes", IEEE Transactions on Biomedical Engineering, Vol. 55, pp. 857–865, 2008.

[14] E. Renard, G. Costalat, H. Chevassus, J. Bringer, "Closed loop insulin delivery using implanted insulin pumps and sensors in type 1 diabetic patients", Diabetes Research and Clinical Practice, Vol. 74, S173–S177, 2006.

[15] E. Ruiz-Velazqueza, R. Femat, D.U. Campos-Delgadoc, "Blood glucose control for type 1 diabetes mellitus: a robust tracking H_∞ problem", Control Engineering Practice, Vol. 12, pp. 1179–1195, 2004.

[16] H.T. Nguyen, N.R. Prasad, C.L. Walker, E.A. Walker, A First Course in Fuzzy and Neural Control, USA, Chapman & Hall/CRC, 2003.

[17] J. Chen, K. Cao, Y. Sun, Y. Xiao, X. Su, "Continuous drug infusion for diabetes therapy: a closed-loop control system design", European Association for Signal Processing Journal on Wireless Communications and Networking, Vol. 2008, Article No. 44, 2008.

[18] C. Li, R. Hu, "Fuzzy-PID control for the regulation of blood glucose in diabetes", Proceedings of the 2009 WRI Global Congress on Intelligent Systems, pp. 170–174, 2009.

[19] M. Ibbini, "A PI-fuzzy logic controller for the regulation of blood glucose level in diabetic patients", Journal of Medical Engineering & Technology, Vol. 30, pp. 83–92, 2006.

[20] M. Ibbini, M. Masadeh, "A fuzzy logic based closed-loop control system for blood glucose level regulation in diabetics", Journal of Medical Engineering & Technology, Vol. 29, pp. 64–69, 2005.

[21] H. Wang, J. Li, Y. Kuang, "Mathematical modeling and qualitative analysis of insulin therapies", Mathematical Biosciences, Vol. 210, pp. 17–33, 2007.

[22] F.V. Bergh, A.P. Engelbrecht, "A study of particle swarm optimization particle trajectories", Information Sciences, Vol. 176, pp. 937–971, 2006.

[23] J. Kennedy, R.C. Eberhart, The Particle Swarm: Social Adaptation in Informal-Processing Systems: New Ideas in Optimization, McGraw-Hill, 1999.

[24] R.C. Eberhart, Y.H. Shi, "Particle swarm optimization: developments, applications and resources", Proceedings of the Congress on Evolutionary Computation, pp. 81–86, 2001.

[25] R. Yang, M. Zhang, T.J. Tarn, "Dynamic modeling and control of a micro-needle integrated piezoelectric micro-pump for diabetes care", 6th IEEE Conference on Nanotechnology, Vol. 1, pp. 146–149, 2006.

[26] H. Modares, A. Alfi, M.B. Naghibi Sistani, "Parameter estimation of bilinear systems based on an adaptive particle swarm optimization", Engineering Applications of Artificial Intelligence, Vol. 23, pp. 1105–1111, 2010.

[27] A. Ratnaweera, S.K. Halgamuge, H.C. Watson, "Self-organizing hierarchical particle swarm optimizer with time-varying acceleration coefficients", IEEE Transactions on Evolutionary Computation, Vol. 8, pp. 240–255, 2004.

[28] H.L. Kwang, First Course on Fuzzy Theory and Applications, Heidelberg, Springer-Verlag, 2005.

[29] M. Al-Fandi, M.A.K. Jaradat, Y. Sardahi, "Optimal PI-fuzzy logic controller of glucose concentration using genetic algorithm", International Journal of Knowledge-Based and Intelligent Engineering Systems, Vol. 15, pp. 99–117, 2011.